International Journal of Pharmaceutics 659 (2024) 124267

Contents lists available at ScienceDirect

International Journal of Pharmaceutics

journal homepage: www.elsevier.com/locate/ijpharm

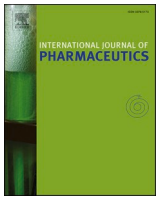

Harnessing therapeutic deep eutectic solvents in self-emulsifying systems to improve CBD delivery

Gennaro Balenzano, Giuseppe Francesco Racaniello, Antonio Spennacchio, Antonio Lopalco, Rosa Maria Iacobazzi, Angela Assunta Lopedota, Valentino Laquintana, Nunzio Denora *

Department of Pharmacy - Pharmaceutical Sciences, University of Bari "Aldo Moro", Via E. Orabona, 4 I-70125, Bari, Italy

ARTICLE INFO

Keywords:
Therapeutic deep eutectic solvents
Self-emulsifying drug delivery systems
Cannabidiol
Oral delivery
Lipid-based formulation
BCS class II

ABSTRACT

In this study, Cannabidiol crystals (CBD) were used as a BCS class II model drug to generate a novel therapeutic deep eutectic solvent (THEDES) with easy preparation using caprylic acid (CA). The hydrogen bonding interaction was confirmed by different techniques such as FT-IR and NMR, resulting in a hydrophobic system suitable for liquid formulations. The CBD-based THEDES, combined with a specific mixture of surfactants and co-surfactants, successfully formed a self-emulsifying drug delivery system (SEDDS) that generated uniform nano-sized droplets once dispersed in water. Hence, the THEDES showed compatibility with the self-emulsifying approach, offering an alternative method to load drugs at their therapeutic dosage. Physical stability concerns regarding the unconventional oily phase were addressed through stress tests using multiple and dynamic light scattering, demonstrating the robustness of the system. In addition, the formulated SEDDS proved effective in protecting CBD from the harsh acidic gastric environment for up to 2 h at pH 1.2. Furthermore, in vitro studies have confirmed the safety of the formulation and the ability of CBD to permeate Caco-2 cells when formulated. This investigation highlights the potential incorporation of THEDES in lipid-based formulations like SEDDS, expanding the avenues for innovative oral drug delivery approaches.

1. Introduction

Deep eutectic solvents (DES) represent a novel approach for different applications in many fields of chemistry, thanks to their tunable and advantageous characteristics with liquid eutectic mixtures obtained from the hydrogen bond interaction between 2 or more components inducing a drastic decrease in their melting point (Zainal-Abidin et al., 2019). In fact, they resulted in low- or nontoxicity, biodegradability, ease of preparation, and inexpensive and readily available raw materials, often belonging to the generally recognized as safe (GRAS) list (Emami and Shayanfar, 2020). Recently, a particular interest in their adoption in the pharmaceutical field as green solvents with high solvency capability has brought an increasing development of new DES, whose properties are influenced by the compounds enrolled in the formation of the hydrogen bond (Smith et al., 2014). Various categories of DES can be identified, including natural DES made from natural raw materials, hydrophobic DES characterized by water immiscibility, supramolecular DES that involves molecules capable of generating supramolecular interactions, and therapeutic DES (THEDES) containing one or more active pharmaceutical ingredients used for DES preparation. In particular, hydrophobic DES and THEDES have been used in more complex systems, such as emulsions and creams for topical application, improving the bioavailability of the drug thanks to the enhanced solubility in these systems (Shah et al., 2023; Van Osch et al., 2020; Wahlgren and Quiding, 2000). This work investigates the possibility of orally delivering a THEDES through the development of a suitable formulation. Among the available drug delivery systems (DDS), self-emulsifying DDS (SEDDS) are an eligible option due to their simple composition and ability to address the dissolution and bioavailability issues of active pharmaceutical compounds that belong to Biopharmaceutics Classification System Class II and IV drugs (Kohli et al., 2010; Tran and Park, 2021). SEDDS can be defined as mixtures of oils, surfactants and cosurfactants that upon contact with an aqueous phase spontaneously emulsify under conditions of gentle agitation. The in situ-generated micro or nanodroplets maintain the delivered drug solubilized in the aqueous environment and enable the transport to the absorptive intestinal epithelium (Knaub et al., 2019; Salawi, 2022). In the last decades, SEDDS have enabled enhanced bioavailability of poorly

* Corresponding author.
E-mail address: nunzio.denora@uniba.it (N. Denora).

https://doi.org/10.1016/j.ijpharm.2024.124267
Received 31 March 2024; Received in revised form 16 May 2024; Accepted 21 May 2024
Available online 24 May 2024

water-soluble drugs, as demonstrated by marketed drugs, such as Sandimmune®/Neoral®, which are presented as preconcentrate encapsulated in soft gel capsules, similarly to many other SEDDS made of liquid or semi-solid lipid excipient (Jannin et al., 2015; Pouton and Porter, 2008).

Herein, the possible applicability and synergy between SEDDS and THEDES used as novel and alternative oily phase was studied. For this purpose, solid-state CBD crystals were selected as a BCS class II model drug for the generation and characterization of a hydrophobic THEDES that allowed to easily reach and overcome the therapeutic dosage of CBD-based commercially available products. The SEDDS was deeply characterized in terms of stability to evaluate the influence of THEDES on the emulsification process. Further, the release behavior from the obtained SEDDS was determined through the distribution coefficient (LogD) between the SEDDS and the release medium and the chemical stability of the loaded CBD was assessed in the simulated GI tract fluids. In the end, via in-vitro biological studies, it was possible to observe the safety profile of the formulation and the ability of CBD to permeate easily through the Caco-2 cells monolayer.

2. Materials and methods

2.1. Materials

Myristic acid ≥ 99 %, Lauric acid ≥ 99 %, Caprylic acid ≥ 99 %, Cremophor EL (PEG-35-castor oil, PEG35-CO), TPGS (D-α-Tocopherol polyethylene glycol succinate), deuterated solvents and HPLC solvents were purchased by Sigma Aldrich Italy (Milan, Italy). Cannabidiol crystals 99 % were purchased by Enecta (Amsterdam, Netherlands). Labrasol ALF (PEG-8 caprylic/capric glycerides), Gelucire 44/14 (lauroyl PEG-32 glycerides), Gelucire 48/16 (PEG-32 stearate), Gelucire 50/13 (PEG-32 hydrogenated palm glycerides) were gifted by Gattefossè Italy (Milano, Italy), Capmul MCM was a gift by Abitec Corporation (Columbus, USA). MilliQ water was obtained through a Milli-Q instrument by Millipore Sigma (Burlington, Massachusetts, USA). For cellular studies, Transwell® permeable supports were from Corning (Corning, NY, USA). Dulbecco's Modified Eagle's medium (DMEM), Dulbecco's phosphate buffered saline, heat-inactivated fetal bovine serum (FBS), L-glutamine (200 mM), penicillin (100 IU/mL), streptomycin (100 mg/mL) and trypsin (2.5 %) were acquired from EuroClone (Italy).

2.2. THEDES formation

THEDES generation was attempted starting from CBD and using fatty acids with increasing numbers of carbon atoms, namely Caprylic Acid (CA), Lauric Acid (LA) and Myristic Acid (MA), following a previously described procedure (Pereira et al., 2019). In particular, the adopted molar ratios are enlisted in Table 1. All the mixtures were heated for 30 min at 50 °C under magnetic stirring at 300 rpm and then equilibrated at 25 °C. The samples that were able to form a clear liquid after this process and remained liquid, in the first instance for 24 h and then for 72 h, as a final control, were considered eligible for further studies.

This procedure could result in the formation of a liquid THEDES (Yes/No) (Table 1), a low melting mixture (LMM) (Table 1) or systems with an overall melting point lower than that of the individual components, which remain solid at room temperature, and are therefore not considered to be DES.

The CA-CBD sample 3:1 accomplished the THEDES formation and was selected as a specimen for the following analysis.

Table 1
Composition and respective molar ratios of the studied components required for generating THEDES.

Components	Molar ratio	THEDES formation
MA – CBD	0.5:1	LMM
	1:1	No
	2:1	LMM
LA – CBD	0.5:1	LMM
	1:1	No
	2:1	LMM
CA – CBD	0.5:1	LMM
	1:1	No
	2:1	LMM
	2.5:1	No
	3:1	Yes

2.3. THEDES density

Density was assessed via gravimetric analysis at 25 °C: 100 μL of the samples were withdrawn using positive displacement pipettes (MICROMAN® E pipette, Gilson Italia, Italy), with disposable capillary piston tips and weighed with an AS 82/220.R2 Analytical Balance. The test was conducted in triplicate.

2.4. Fourier transformed-infrared spectroscopy (FT-IR)

FT-IR was used as first methodology to investigate the interaction between CBD and CA. For the analysis, KBr pellets (2 % of sample) were analyzed by FT-IR 1600 PerkinElmer spectrophotometer. Data were acquired between 4000 cm^{-1} and 400 cm^{-1}.

2.5. Nuclear magnetic resonance (NMR)

NMR spectroscopy was used to further confirm the establishment of hydrogen-bonding interactions between CBD and CA. Experiments were performed on samples made of at least 50 % v/v of CA or THEDES in d_6-DMSO and alternatively 30 % w/v of CBD in d_6-DMSO. The spectra were recorded using an Agilent VNMRS 500 MHz spectrometer, and ^{1}H NMR spectra were analyzed using the residual solvent signal of d_6-DMSO at 2.50 ppm (Fulmer et al., 2010).

2.6. Thermogravimetric analysis (TGA)

TGA was performed to verify THEDES stability at increased temperatures with a PerkinElmer Thermogravimetric Analyzer Pyris 1 TGA. An open platinum pan was calibrated at the temperature of 25 °C and the samples were placed within it. Thereafter, the prepared pan was suspended in the furnace. The weight of the sample was recorded during heating from 25 to 600 °C at a heating rate of 10 °C/min, starting from an initial weight of the sample of 10 – 15 mg. Nitrogen flow was imposed at 30 mL/min.

2.7. SEDDS preparation

To produce SEDDS samples, the prepared THEDES, surfactants and co-surfactants were combined at different ratios and mixed using an Eppendorf ThermoMixer F® (Eppendorf, Italy) until a uniform translucent phase was obtained. The composition of the 24 prepared samples and relative data are presented in **Table S1**. Then, to evaluate the self-emulsifying properties, 50 μL of the resulting SEDDS preconcentrates were dispersed in 5 mL of distilled water at 37 °C (1 % v/v). Visual inspection of all samples was performed to exclude macroemulsions characterized by a non-transparent, milky appearance, before determining the average particle size and PDI using a Zetasizer Nano ZS (Malvern Instruments Ltd., UK). Phase separation was tested for both SEDDS preconcentrate and dispersed SEDDS via centrifugation for 30 and 10 min, respectively, at 10,000 rcf, to exclude any physical instability issue (Zupančič et al., 2017). The formulation composed by the 30 % v/v of THEDES, 40 % v/v of PEG35-CO, 20 % v/v of Labrasol ALF and 10 % v/v of ethanol was selected was selected for further studies. The samples were measured in triplicate.

2.8. Cloud point determination

The Cloud Point of the generated emulsion was determined as first prerequisite of the thermal stability analysis of the generated emulsion (Agrawal et al., 2015; Gardouh et al., 2020). The SEDDS preconcentrate was diluted (1:100) with distilled water and gradually warmed (0.5 °C/min). Optical phenomena, drug precipitation or phase separation were examined by multiple light scattering (MLS) increasing the temperature starting from 25° C. The analysis was conducted using Turbiscan LAB instrument (Formulaction, FR) and analyzed with TurbiSoft Lab 2.3.1.125.

2.9. SEDDS stability to pH variation and dilution

The SEDDS preconcentrate was evaluated in terms of stability against physiological pH variation in the GI tract and consequently to dilution using a gastrointestinal simulation system (Broesder et al., 2021; Schellekens et al., 2007). Briefly, SEDDS preconcentrate was allowed to emulsify with an initial concentration of 2 % v/v in a simulated gastric environment using HCl pH 1.2 at 37 °C. Then, following the parameters in Table 2, the fluid was modified to check the overall stability of the emulsion in the GI tract and reach a final concentration of SEDDS in the simulated fluid of 1 % v/v.

The sample analysis was followed by size and PDI determination using Zetasizer Nano ZS (Malvern Instruments Ltd., UK) and investigating the variation of the Turbiscan stability index (TSI) for each pH and dilution zone. This parameter was obtained using Turbiscan LAB instrument (Formulaction, FR) and TurbiSoft Lab 2.3.1.125 software using **Equation (1).**

$$TSI(t) = \frac{1}{N_h} \sum_{t_i=1}^{t_{max}} \sum_{z_i=z_{min}}^{z_{max}} |BST(t_i, z_i) - BST(t_i - 1, z_i)| \quad (1)$$

with: t_{max} the measurement point corresponding to the time t at which the TSI is calculated, z_{min} and z_{max} the lower and upper selected height limits respectively, $N_h = (z_{min}\text{-}z_{max})\ /\Delta h$ the number of height positions in the selected zone of the scan and BST the considered signal (Back Scattering if Trasmittance < 0.2 %, Trasmittance otherwise). Consequently, the sample is stable when the TSI tends toward zero and unstable when the TSI is very high. Note that the TSI is equal to zero for t = 0

2.10. HPLC method

To quantify CBD, a slightly modified HPLC method was adapted from Fraguas-Sánchez et al. (2020) using Shimadzu HPLC Nexera series, equipped with SPD-M40 photodiode array detector, SIL-40C autosampler and CTO-40C column oven. As stationary phase a Zorbax Eclipse C18 plus 150 × 45 mm pore size 5 μm with a guard column was used, while MeOH:ACN:H_2O adjusted with acetic acid at pH 4.5 (45:30:25) as the mobile phase at 0.9 mL/min, λ = 228 nm. The calibration curve was obtained in a range of concentration between 1.90x10^{-2} and 1.90 mM (R^2 = 0.9996).

2.11. $LogD_{SEDDS/release\ medium}$

$LogD_{SEDDS/release\ medium}$ was determined to evaluate the release of CBD from SEDDS, according to Bernkop-Schnürch and Jalil (2018). This parameter represents a more informative value regarding the in vivo drug release behavior from SEDDS than in vitro drug release profiles. $LogD_{SEDDS/release\ medium}$ was then calculated using **Equation (2)**, assessing the maximum solubility in SEDDS preconcentrate without the ethyl alcohol, which is more likely to be released instantly from the SEDDS once administered, and in PBS 50 mM at pH 6.8 prepared according to Italian Official Pharmacopoeia XII edition (2008) set as simulated release media (Bonengel et al., 2018; Jörgensen et al., 2020).

$$LogD_{SEDDS/Release\ medium} = \log\left(\frac{maximum\ solubility\ of\ CBD\ in\ SEDDS}{maximum\ solubility\ of\ CBD\ in\ PBS\ pH\ 6.8}\right) \quad (2)$$

2.12. CBD stability in GI simulating fluid

Following the previously described protocol in section 2.9, the chemical stability of CBD was evaluated. In particular, after the emulsification of SEDDS preconcentrate, withdrawals of 150 μL from the sample were performed for each pH interval and analyzed with HPLC after proper dilution. The data were analyzed as the remaining percentage of CBD in solution and calculated as described in **Equation (3)**.

$$\%remainingCBD = \frac{CBDsampleconcentration}{InitialCBDconcentration} \times 100 \quad (3)$$

2.13. Cytotoxicity assay

Potential cytotoxic effects of CBD, CBD-loaded and unloaded SEDDS were evaluated by MTT (3-(4,5-dimethylthiazol-2-yl)-2,5-diphenyltetrazolium bromide) assay on Human colorectal carcinoma cell lines (Caco-2) as previously described (Arduino et al., 2024; Depalo et al., 2017). This assay is based on the measurement of mitochondria activity of living cells to convert water-soluble MTT into water-insoluble formazan crystals. Briefly, Caco-2 cells were plated into a 96 wells plate in a concentration of 5 × 10^3 cells/well in 100 μL of high-glucose Dulbecco's modified Eagle's medium (DMEM) supplemented with 10 % (v/v) fetal bovine serum (FBS), 1 % (v/v) l-glutamine, 1 % (v/v) penicillin/streptomycin. Cells were incubated for 24 h at 37 °C in a humidified atmosphere and 5 % CO_2 environment. Afterward, the cells were treated with 100 μL of samples dissolved in DMEM for 6, 24 and 72 h. Three conditions were tested at different concentrations, in particular CBD-loaded SEDDS, prepared as described in section 2.7 (CBD-SEDDS), unloaded SEDDS (SEDDS), and CBD dissolved in DMSO mimicking the amount of drug in CBD-SEDDS (CBD). The tested concentration for each condition was obtained by diluting the samples in complete cell culture media at 0.1 %, 0.05 %, 0.025 % and 0.01 % (v/v). Untreated cells were employed as a positive control. The experiment was performed in triplicates. Cell viability was calculated using the following **Equation (4)**:

$$\%Viability = \frac{AverageAbsorbanceofeachsampletriplicate}{AverageAbsorbanceofpositivecontrol} \times 100 \quad (4)$$

Results were expressed as % cell viability at each tested dose.

2.14. In vitro permeation studies

To evaluate the effectiveness of CBD-SEDDS in enhancing drug permeation, we conducted apical to basolateral (P_{app}, AP) permeability

Table 2
Parameters for the simulated GI tract fluid adopted for the stability tests.

Phase	Initial pH	Volume (mL)	Time (h)	Switch Solutions	Final pH
Stomach	1.2	500	2.0		
Jejunum	1.2	629	2.0	4.08 g KH_2PO_4, 30 mL NaOH 2.0 M (80 g/L), demineralized water of 129 mL	6.8
Ileum (distal)	6.8	940	0.5	2.04 g KH_2PO_4, 12.0 mL NaOH 2.0 M (80 g/L), demineralized water of 311 mL	7.5
Colon (proximal)	7.5	1000	1.5	9 mL HCl 3.0 M, demineralized water of 60 mL	6.0

studies on Caco-2 cells. as previously reported (Pisani et al., 2019; Roger et al., 2017). Cells were seeded at a density of 100,000 cells/cm^2 on 12-well polyester Transwell inserts (pore size 0.4 μm, diameter 12 mm, apical volume 0.5 mL, basolateral volume 1.5 mL). At first, the Caco-2 cell barrier function was verified through *trans*-epithelial electrical resistance (TEER) using an EVOM apparatus and through the measurement of the flux of the paracellular standard fluorescein isothiocyanate-dextran (FD4, Sigma-Aldrich Merck Italy, Milano, Italy) (200 μg/mL) and the transcellular standard diazepam (75 mM). Cells were equilibrated in DPBS as transport medium. At time 0, the culture medium was aspirated from both the apical (AP) and basolateral (BL) chambers of each insert, and the cell monolayers were washed three times (10 min per wash) with Dulbecco's phosphate-buffered saline (DPBS) pH = 7.4. Finally, a solution of compounds diluted in DPBS was added to the apical or basolateral chamber. For AP-to-BL flux studies, the samples were added to the apical chambers. The CBD was first dissolved in DMSO and then diluted with the test medium, while SEDDS were dispersed in the medium before the analysis. The tested solutions were then added to the donor side (500 μL for the AP chamber), and a fresh assay medium was added to the receiver compartment. The DMSO in the samples never exceeded 1 % (v/v). Transport experiments were performed under cell culture conditions (37 °C, 5 % CO_2, 95 % humidity) at a concentration of the samples of 0.025 % v/v. After an incubation period of 120 min, samples were taken from the apical and basolateral sides of the monolayer and stored until further analysis. A quantitative analysis of CBD in the tested samples was performed using the HPLC method reported above. Each sample was tested in triplicate, and experiments were repeated three times. The apparent permeability, in units of cm/sec, was calculated using the following **Equation (5)**:

$$P_{app} = \left(V_a / Area \times time \right) \times \left([CBD]_{acceptor} / [CBD] \right) \quad (5)$$

where "V_a" is the volume in the acceptor well, "*Area*" is the surface area of the membrane, "*time*" is the total transport time, "$[CBD]_{acceptor}$" is the concentration of the drug measured using HPLC, and "$[CBD]_0$" is the initial drug concentration in the AP chamber.

2.15. Statistical analysis

Results were expressed as the mean ± SD from three independent experiments and analyzed using GraphPad Prism version 5.0 to calculate the significance between groups using paired *t*-test method and two-way analysis of variance (ANOVA) followed by the Bonferroni post hoc tests. Data are indicated with *** $p < 0.001$.

3. Results and discussion

3.1. THEDES formation and characterization

The systematic approach based on evaluating CA, LA and MA as candidate compounds suitable for hydrogen bond interaction could be justified by the structural analogy between CBD and some terpenic compounds (Fig. 1). In fact, fatty acids have already been reported as valuable components for the generation of hydrophobic DES, in particular with terpene compounds (Arcon and Franco, 2020; Barani Pour et al., 2022; Kyriakoudi et al., 2022; Pereira et al., 2019; Tang et al., 2018). Further, the enrolment of CBD, an active pharmaceutical ingredient, in the eutectic mixture allowed to define it as a hydrophobic THEDES. Regarding the examined molar ratios, none of the samples with twice the moles of CBD when compared to the fatty acid (molar ratio 0.5:1) managed to form a liquid phase, independently from the hydrocarbon chain length. Evaluation of LA-CBD and MA-CBD samples with 1:1 and 2:1 M ratios highlighted the formation of LMM liquid when warmed at higher temperatures, but solidification occurred once cooled at RT. This aspect is in contrast with DES which remain liquid at RT and it could be possible to consider DES as LMM with an even lower melting point. In fact, the decreased melting point is induced by hydrogen bonding formation for both DES and LMM (de Oliveira Vigier and García-Álvarez, 2017; Rengstl et al., 2014). Hypothetically, the demonstrated interaction obtained for these combinations of compounds was not able to decrease the melting point of CBD from about 60 °C to 25 °C as well as the one of LA and MA, 44–46 °C and 54 °C respectively. For what concerns CA-CBD, although the first two attempted molar ratios of 1:1 and 2:1 accomplished the generation of DES, after 24 h the appearance of the samples was evaluated and they were excluded for not maintaining a complete liquid state. However, the ratios of CA-CBD 2.5:1 and 3:1 exhibited a liquid state for over 24 h. Nonetheless, conducting further stability checks at 72 h, the 2.5:1 ratio of CA-CBD was subsequently excluded, prompting the focus to shift to the sample with a 3:1 ratio of CA-CBD. The measured density for this sample was 0.882 g/mL.

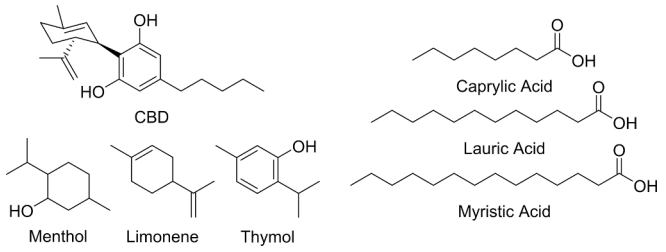

Fig. 1. Chemical structure of CBD and terpenes similar to CBD moiety. On the right, the structure of the fatty acids.

Hydrogen bonding and thereafter DES generation was assessed through FT-IR and NMR as techniques already established in the literature for these pursues (Abri et al., 2019a; Jurić et al., 2021).

As shown in Fig. 2, the spectra relative to CBD presented all the characteristic peaks at 3410 and 3521 cm^{-1} relative to the stretching of the O–H group, 3073 cm^{-1} relative to C–H of the aromatic ring as well as the vibrational stretching at 1623 cm^{-1}, 1582 cm^{-1}, 1514 cm^{-1} and 1443 cm^{-1} relative to the backbone of the aromatic ring. Other relevant peaks regarded the aromatic C-O at 1214 cm^{-1} and the bending of methyl-group at 1375 cm^{-1} (Li et al., 2021). Spectra of CA showed as characteristic peaks the stretching of C = O at 1712 cm^{-1}, the vibrational stretching of C − O and the bending of O − H at 1458, 1413, and 1379 cm^{-1}. From the analysis of THEDES, an expansion and shifting towards longer wavelengths are observed in the signals related to the aromatic OH groups of CBD. These signals converge into a broad peak at 3451 cm^{-1}, indicative of hydrogen bond formation, as reported in the literature (Busato et al., 2021; Ghaedi et al., 2017; Haider et al., 2021). Similarly, a reduction in intensity is noticeable in the signal associated with the C = O stretching of octanoic acid at 1712 cm^{-1}, a functional group that could serve as a hydrogen bond acceptor. Furthermore, leftward shifts are evident in the peaks corresponding to the aromatic stretching of methylene groups of CBD between 1630 and 1400 cm^{-1}. These shifts, though of lesser significance in the analysis, suggest hydrogen bond formation, leading to a variation in electron density on the aromatic ring. The general preservation of all the relevant peaks was considered as first evidence of the structural preservation of the compounds during the THEDES generation process.

Further confirmation regarding the establishment of hydrogen bonding interactions was provided through the analysis of ^{1}H NMR spectra in Fig. 3. It was possible to identify three regions of major interest based on the significant shifts in terms of ppm.

In particular, the deshielded signal in the THEDES of the proton in alpha of the carboxylic group (proton 1) could be attributed to the presence of interaction, as well as for the protons in the region between 4.5 and 5.6 ppm relative to the double bonds of CBD (proton 3, 4, 5). In detail, the proton 5 upshift may be explained by hydrogen bond interaction, whereas hypothetically, protons 3 and 4 experienced a downshift

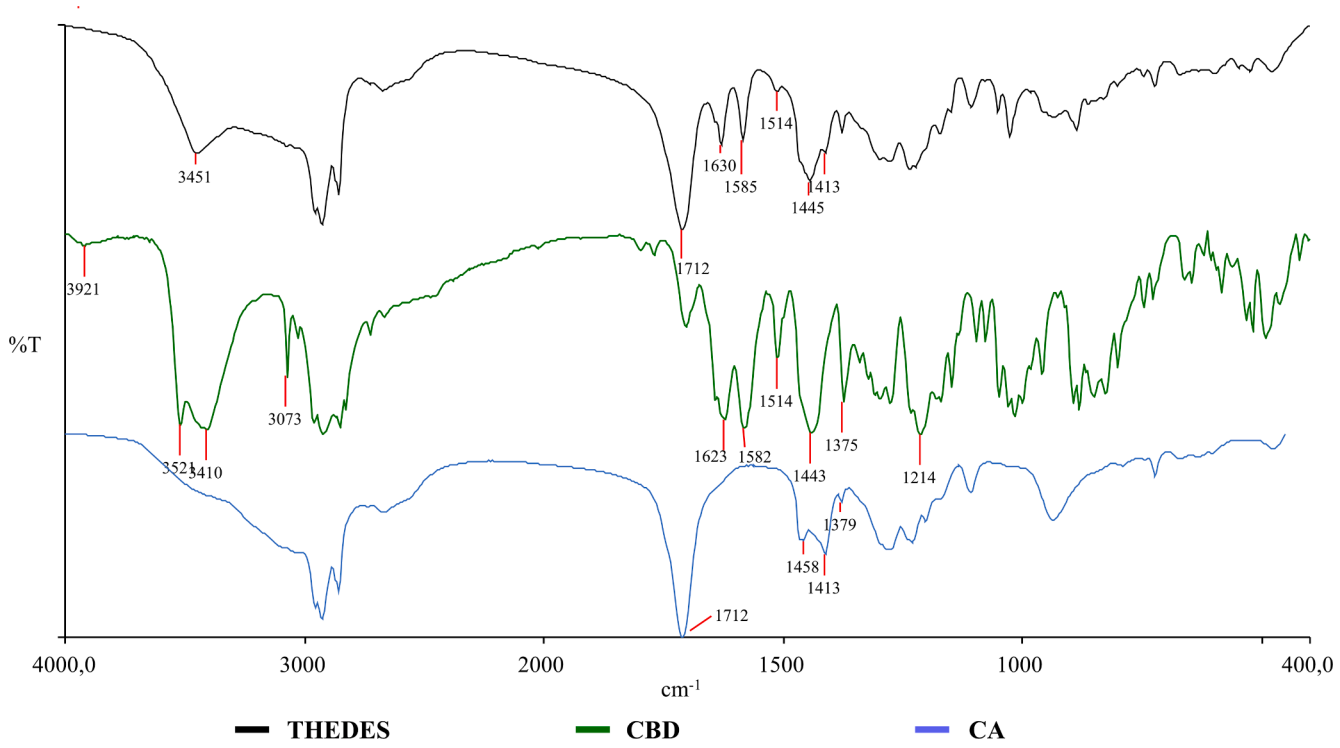

Fig. 2. FT-IR spectra for THEDES, CBD and CA.

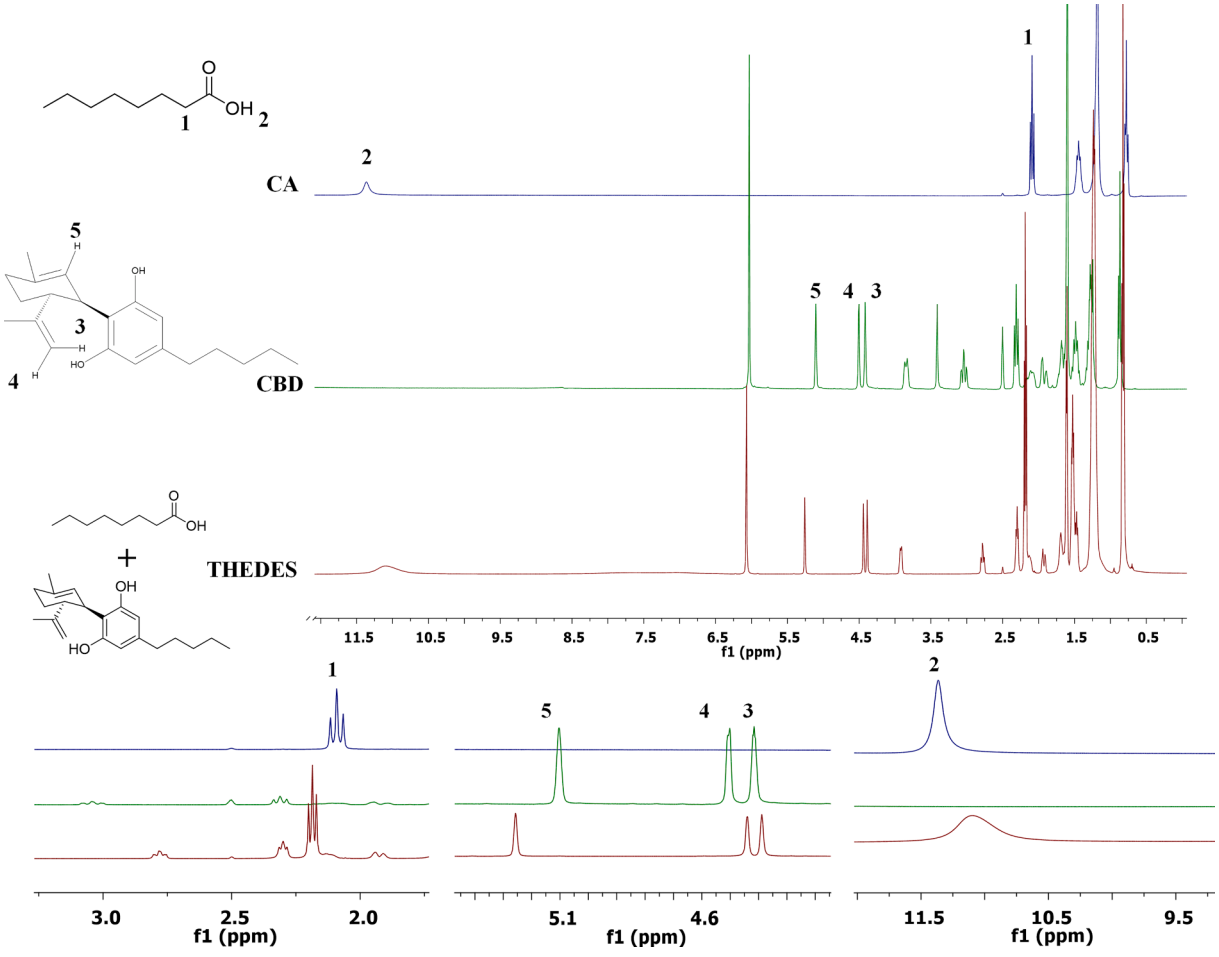

Fig. 3. ^{1}H NMR spectra for CA, CBD and THEDES with their relative zoom on the significant peaks.

due to loss of interaction with the solvent (d-DMSO) and the loss intramolecular ones due to the formation of THEDES and the presence of CA among the different molecules (Charisiadis et al., 2014; Schaeffer et al., 2021). This confirms the primary hypothesis that the structural similarity among some CBD moieties and terpene allowed to obtain a eutectic mixture. In the end, the carboxylic proton of CA at 11.4 ppm, once analyzed as THEDES became a broad peak, further indication of hydrogen bond formation (Abri et al., 2019b).

The THEDES was last analyzed through TGA, the results, shown in Fig. 4, demonstrated the stability of the obtained eutectic system in the range of the working temperature. Furthermore, the presence of different T_{onset} for THEDES is aligned with the general thermograms already present in the literature, with the observed degradation characterized by the first loss of CA and then of the CBD (González-Rivera et al., 2022).

3.2. SEDDS preparation

SEDDS were prepared using the generated THEDES as a novel oily phase, capable of reaching and overcoming the drug dosage loaded in Epidiolex®, the commercially available product with 100 mg/mL of CBD without the use of cosolvents. The first step was a systematic analysis of the compatibility of THEDES with surfactants known for their self-emulsification properties, namely PEG35-CO and Gelucire 48/16. The preliminary analysis showed Gelucire 48/16 as a possible candidate for SEDDS formulation, but the samples present in **Table S1** were excluded for the observed PDI indicating a non-homogenous population. Furthermore, these samples lacked long-term physical emulsion stability with an observed phase separation of the SEDDS from the dispersing phase, due to the formation of macro-sized visible droplets. Nevertheless, it is noteworthy that the influence of cosolvents, such as ethanol, in the self-emulsification process improves the PDI parameter when adopted thanks to their ability to further reduce the oil–water interfacial tension (Içten et al., 2017; Jörgensen et al., 2020). Conversely, samples containing PEG35-CO were unable to directly self-emulsify properly when mixed with only THEDES, but it was selected as surfactant because often used in SEDDS formulations and was shown previously to form stable emulsions at a concentration of 30–40 % (Lam et al., 2021) and for being generally considered as safe and biocompatible (Zaichik et al., 2019). As the final excipient, Labrasol® ALF was selected for being already documented useful co-surfactant and permeation enhancer capable of improving intestinal absorption (Eaimtrakarn et al., 2002, McCartney et al., 2019, Sha et al., 2005).

Among all the samples, the formulations composed of 30 % v/v of THEDES, 40 % v/v of PEG35-CO, 20 % v/v of Labrasol ALF and 10 % v/v of ethanol demonstrated the best emulsion characteristic when dispersed with droplet size of 100.2 nm and the observed PDI of 0.252, below the limit parameter of 0.3 advantageous for emulsion stability (Cardona et al., 2019). On the other hand, the remaining samples were excluded for their high polydispersity. The following studies were conducted on this sample also for the greater amount of THEDES adopted in it and, therefore, the larger amount of drug that could be delivered with a reduced quantity of formulation. Stability studies of the formulation via centrifugation were all passed without any observation of separation phenomena.

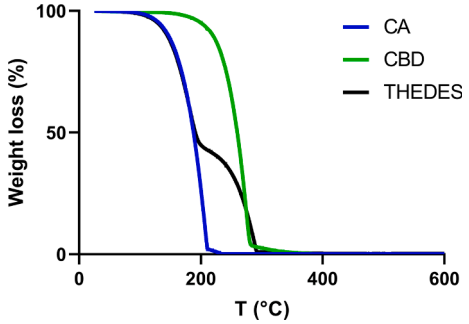

Fig. 4. Acquired thermogravimetric curves for CA, CBD and THEDES.

Thanks to the use of THEDES as a novel oily phase, the therapeutic dosage was reached by loading 100 mg of CBD in 900 μL of SEDDS and the release behavior of the drug from SEDDS can be predicted by the distribution coefficient, calculated from the ratio of the drug solubility in SEDDS preconcentrate and the release medium (Bernkop-Schnürch and Jalil, 2018). The obtained values were used to calculate a $LogD_{SEDDS/release\ medium}$ of 4.92, aligned with the already high lipophilicity of CBD (XlogP3-AA = 6.5, Computed by XLogP3 3.0 (PubChem release 2021.10.14)). Bernkop-Schnürch and Jalil (2018) suggested that drug-loaded SEDDS systems with $LogD_{SEDDS/release\ medium}$ up to 2 can retain CBD in the oily phase without immediately releasing it, therefore protecting the drug from the external environment and precipitation phenomena. Additionally, a $LogD_{SEDDS/release\ medium} > 3$ significantly improves the in vivo-in vitro correlation, which was demonstrated to be a soft spot for SEDDS formulation (Park et al., 2020).

3.3. Cloud point

This analysis assessed the T_{Cloud} value, as the limit temperature before emulsion destabilization and it was measured to evaluate the impact of temperature on the phase behavior of optimized dispersed SEDDS. For this reason, starting from room temperature the temperature was increased until evidence of destabilization processes were observed through MLS. As shown in Fig. 5, the emulsion resulted stable until the temperature of 45° C, 40 min after the beginning of the analysis, the increasing deviations in terms of transmittance and back-scattering suggested the increasing turbidity of the sample. As a result, T_{Cloud} was above the physiological temperature and the preconcentrate was considered eligible as DDS.

3.4. SEDDS stability in GI simulating fluid

In Table 3, the stability of the emulsion at different pH was evaluated through the complementary analysis of two parameters regarding the size and PDI of the droplet obtained from the SEDDS formulation and the TSI value calculated from the TurbiscanLab (Lopedota et al., 2021). The data on the dimension of the droplets demonstrated good stability of the emulsion in the significant ranges of pH 1.2 and 6.8, where the SEDDS are intended to protect CBD from the harsh stomach pH and then allow it to reach the small intestine. This hypothesis was further confirmed by the TSI value that is significantly below 10, which is the limit value for emulsion systems ("Turbiscan Stability Index: The Criteria and Correlation to Visual Observation," n.d.).On the other hand, instability phenomena were detectable at pH 7.4 with a PDI value of 0.39 suggesting an increased dispersity in terms of the size of droplets' population. The TSI value was unable to reveal this evidence, possibly due to the little significance during the 30 min at pH 7.4.

Similarly, the chemical stability of CBD in the SEDDS formulation was investigated in the simulated GI tract fluid, focusing on the possibility of protecting the drug from the acidic pH of the stomach. In fact, CBD was found to be highly unstable at low pH values, with significant drug loss that can reach 98 % due to CBD conversion in multiple products (Merrick et al., 2016; Watanabe et al., 2007). As shown in Table 3, the obtained SEDDS demonstrated to guarantee the maintenance of the drug stable passing through low pH value of 1.2 to pH 6.8. This result was in agreement with the previously recorded $LogD_{SEDDS/release\ medium}$ value, which suggested the permanence of the drug in the SEDDS without leakage of the drug from them.

3.5. Cytotoxicity assay and in vitro permeability studies

The performed MTT assay was used to determine if the developed

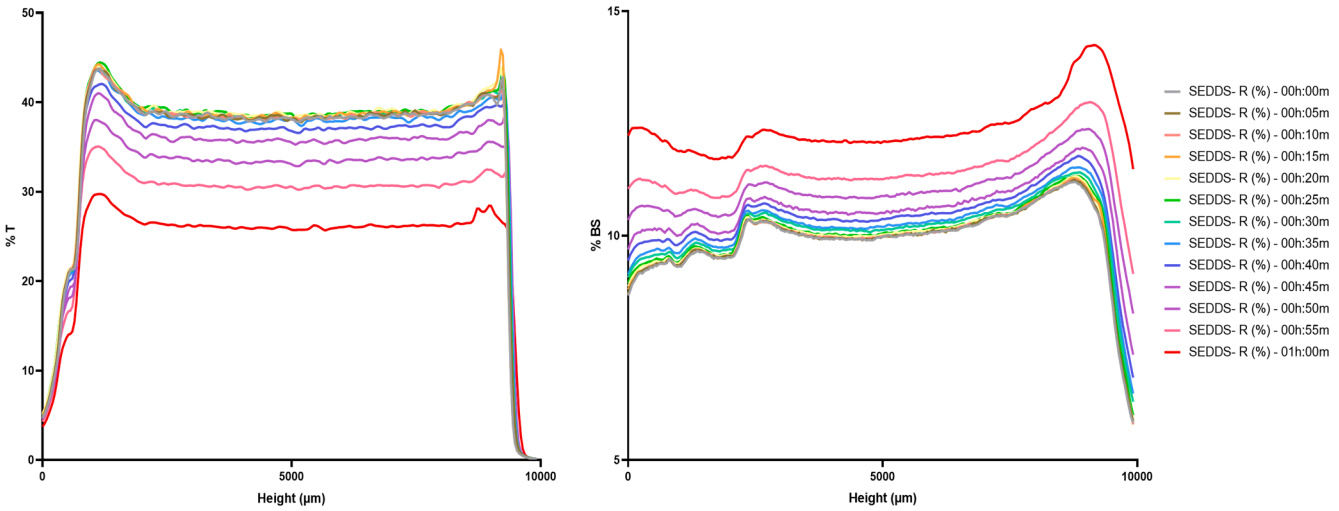

Fig. 5. Transmittance (%T) and Back scattering (% BS) variation at different time points. On the X-axis the "Height" refers to the point of the analyzed vial from the base to the top.

Table 3
The maximum recorded TSI value for each pH interval was intended as the stability index, as well as the dimensions and PDI of the generated emulsion.

pH value	TSI value	Droplet parameter		% remaining CBD
		Size (nm)	PDI	
1.2	1.03	85.1	0.28	99.2
6.8	2.99	79.8	0.27	98.7
7.4	0.18	88.6	0.39	98.5
6	5.65	71.2	0.23	98.1

formulation affected the viability of Caco-2 cells, used as model cell line to mimic the intestinal barrier (Bu et al., 2016). The obtained data (Fig. 6) were analyzed considering cell viability of at least 80 % as non-toxic, within 80–40 % as weakly/moderately and below 40 % as strongly cytotoxic (López-García et al., 2014). Notably, previous studies demonstrated CBD repression of Caco-2 cell viability inducing apoptotic cell death via CB2 receptor-mediated mechanism, while not being toxic in normal human cells (Lee et al., 2022). In this regard, as shown in Fig. 6, the reduced viability is manifested in a dose-dependent manner, with the percentage of viability below 40 % at the higher concentrations and CBD-SEDDS significantly more effective than free CBD mainly after 24–72 h of treatment at 0.025 and 0.01 % v/v. On the other hand, the SEDDS simple mixture of the excipients did not exhibit the same behavior with tolerable to non-toxic results starting from the 0.05 % (v/v) concentration. As a consequence, the hypothesis that best explains the ability of CBD-SEDDS to reduce the viability rate of Caco-2 is its performance as a DDS since the potential cytotoxic effect derives from CBD successfully reaching the cell membrane and interacting with the CB2 receptors. Furthermore, starting from the comparison of the different evaluated time points, the viability repression effect was influenced by two parameters: time of exposure and CBD concentration. In fact, after 6 h, the CBD-SEDDS sample overlay the viability profile of CBD, while viability under the 20 % was observed after 24 h even at lower concentrations, with an even lower percentage reached for the 72 h time point, suggesting the accomplishment of the maximum possible effect in the set experimental conditions. Nevertheless, as the protective mucus layer of the intestinal epithelium is not considered in this experimental setup, in vitro results may not correctly reflect in vivo conditions. Additionally, it is also important to consider that due to the processes involved in digestion and absorption, the concentration of SEDDS in vivo could gradually decrease over time (Claus et al., 2023).

Following these results, in vitro permeation studies were performed at 0.025 % CBD-SEDDS and CBD in DMSO concentration incubating cells just for 2 h. The P_{app}AP values in Table 4 show a 1000-fold improvement in CBD permeability, highlighting the enhancement

Table 4
Calculated P_{app}AP values for the AP-to-BL permeation of CBD across Caco-2 monolayer.

Compounds	P_{app}AP (cm/sec)
CBD	$9.4 \times 10^{-9} \pm 0.5 \times 10^{-9}$
SEEDS-CBD	$6.0 \times 10^{-6} \pm 4.8 \times 10^{-7}$
Diazepam	$7.7 \times 10^{-5} \pm 0.2 \times 10^{-5}$
FD4	$0.22 \times 10^{-5} \pm 0.03 \times 10^{-5}$

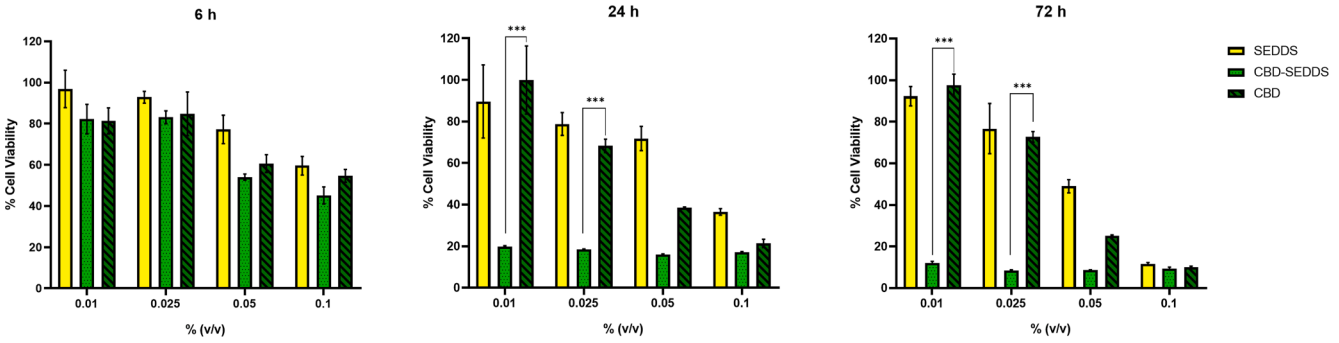

Fig. 6. Results of MTT assay on Caco-2 cells after 6, 24 and 72 h incubation at different % v/v concentrations of CBD, CBD-loaded and unloaded SEDDS. Results are expressed as mean ± S.D. of three experiments. A difference was considered to be very significant with *** $p < 0.0001$.

achieved through formulating CBD in a lipid-based SEDDS formulation (*** $p < 0.0001$). Furthermore, these results seem very promising in terms of achieving higher bioavailability of the drug after oral administration. The values obtained for the paracellular standard FD4, and the transcellular standard diazepam, were in agreement with those previously reported in the literature (Pisani et al., 2019).

4. Conclusions

In this work, CBD was adopted as a model drug for the generation of a novel THEDES characterized by an easy preparation using CA and the hydrogen bond interaction was confirmed by the adoption of different spectroscopic techniques. Hence, it was possible to generate a hydrophobic system useful for the liquid delivery of drugs hypothetically ready to be included in more complex formulations. The investigated system composed of the CBD-based THEDES and a proper mixture of surfactants and co-surfactants successfully generated a SEDDS preconcentrate able to produce a monodisperse nano-sized droplet population. The THEDES was therefore compatible with the self-emulsifying approach and could represent an alternative approach in guaranteeing the achievement of the therapeutic dosage. Possible stability issues of the obtained emulsion relative to the adoption of a non-usual oily phase were taken into account and all the stress tests were passed with the double-checked system of multiple and dynamic light scattering. Furthermore, the formulation resulted in a useful tool for the protection of CBD from the harsh acidic gastric environment, protecting the drug for 2 h at pH 1.2. Moreover, via in-vitro biological studies, it was possible to observe the safety profile of the formulation and the ability of CBD to permeate easily through Caco-2 cells monolayer when formulated. In conclusion, this preliminary study demonstrated the feasibility of integrating hydrophobic THEDES, into lipid-based formulations like SEDDS, thereby broadening the horizons of drug delivery systems.

CRediT authorship contribution statement

Gennaro Balenzano: Writing – review & editing, Writing – original draft, Visualization, Methodology, Investigation, Conceptualization. **Giuseppe Francesco Racaniello:** Visualization, Methodology, Investigation. **Antonio Spennacchio:** Writing – review & editing, Methodology. **Antonio Lopalco:** Methodology, Writing – review & editing. **Rosa Maria Iacobazzi:** Writing – review & editing, Investigation. **Angela Assunta Lopedota:** Writing – review & editing, Methodology. **Valentino Laquintana:** Supervision, Methodology, Investigation. **Nunzio Denora:** Writing – review & editing, Supervision, Funding acquisition, Conceptualization.

Declaration of competing interest

The authors declare that they have no known competing financial interests or personal relationships that could have appeared to influence the work reported in this paper.

Data availability

Data will be made available on request.

Acknowledgments

Gennaro Balenzano is supported by Italfarmacy srl (Trani, Italy). Authors acknowledge Farmalabor srl. (Canosa di Puglia, Italy), Centro Studi e Ricerche “Dr. S. Fontana 1900-1982” (Canosa di Puglia, Italy) for their technical support. Authors thank Mr. Nicola Di Masi (University of Bari, Bari, Italy) for his skillful technical assistance in recording NMR spectra. The University of Bari “Aldo Moro” (Bari, Italy) is also gratefully acknowledged for its financial support.

Appendix A. Supplementary material

Supplementary data to this article can be found online at https://doi.org/10.1016/j.ijpharm.2024.124267.

References

Abri, A., Babajani, N., Zonouz, A.M., Shekaari, H., 2019a. Spectral and thermophysical properties of some novel deep eutectic solvent based on l-menthol and their mixtures with ethanol. J. Mol. Liq. 285, 477–487. https://doi.org/10.1016/j.molliq.2019.04.001.

Abri, A., Babajani, N., Zonouz, A.M., Shekaari, H., 2019b. Spectral and thermophysical properties of some novel deep eutectic solvent based on l-menthol and their mixtures with ethanol. J Mol Liq 285, 477–487. Doi: 10.1016/j.molliq.2019.04.001.

Agrawal, A.G., Kumar, A., Gide, P.S., 2015. Formulation of solid self-nanoemulsifying drug delivery systems using *N* -methyl pyrrolidone as cosolvent. Drug Dev. Ind. Pharm. 41, 594–604. https://doi.org/10.3109/03639045.2014.886695.

Arcon, D.P., Franco, F.C., 2020. All-fatty acid hydrophobic deep eutectic solvents towards a simple and efficient microextraction method of toxic industrial dyes. J. Mol. Liq. 318, 114220 https://doi.org/10.1016/j.molliq.2020.114220.

Arduino, I., Di Fonte, R., Tiboni, M., Porcelli, L., Serratì, S., Fondaj, D., Rafaschieri, T., Cutrignelli, A., Guida, G., Casettari, L., Azzariti, A., Lopedota, A.A., Denora, N., Iacobazzi, R.M., 2024. Microfluidic development and biological evaluation of targeted therapy-loaded biomimetic nano system to improve the metastatic melanoma treatment. Int. J. Pharm. 650, 123697 https://doi.org/10.1016/j.ijpharm.2023.123697.

Barani Pour, S., Jahanbin Sardroodi, J., Rastkar Ebrahimzadeh, A., 2022. Structure and dynamics of hydrophobic deep eutectic solvents composed from terpene-fatty acids investigated by molecular dynamics simulation. J. Mol. Graph. Model. 114, 108180 https://doi.org/10.1016/j.jmgm.2022.108180.

Bernkop-Schnürch, A., Jalil, A., 2018. Do drug release studies from SEDDS make any sense? J. Control. Release 271, 55–59. https://doi.org/10.1016/j.jconrel.2017.12.027.

Bonengel, S., Jelkmann, M., Abdulkarim, M., Gumbleton, M., Reinstadler, V., Oberacher, H., Prüfert, F., Bernkop-Schnürch, A., 2018. Impact of different hydrophobic ion pairs of octreotide on its oral bioavailability in pigs. J. Control. Release 273, 21–29. https://doi.org/10.1016/j.jconrel.2018.01.012.

Broesder, A., Berends, J.M.E., Scheepers, S.M., Nguyen, D.N., Frijlink, H.W., Hinrichs, W. L.J., 2021. Ileo-colon targeting of the poorly water-soluble drug celecoxib using a pH-dependent coating in combination with self-emulsifying drug delivery or solid dispersion systems. Pharmaceutics 13, 731. https://doi.org/10.3390/pharmaceutics13050731.

Bu, P., Narayanan, S., Dalrymple, D., Cheng, X., Serajuddin, A.T.M., 2016. Cytotoxicity assessment of lipid-based self-emulsifying drug delivery system with Caco-2 cell model: Cremophor EL as the surfactant. Eur. J. Pharm. Sci. 91, 162–171. https://doi.org/10.1016/j.ejps.2016.06.011.

Busato, M., Di Lisio, V., Del Giudice, A., Tomai, P., Migliorati, V., Galantini, L., Gentili, A., Martinelli, A., D'Angelo, P., 2021. Transition from molecular- to nano-scale segregation in a deep eutectic solvent - water mixture. J. Mol. Liq. 331 https://doi.org/10.1016/j.molliq.2021.115747.

Cardona, M.I., Nguyen Le, N.-M., Zaichik, S., Aragón, D.M., Bernkop-Schnürch, A., 2019. Development and in vitro characterization of an oral self-emulsifying delivery system (SEDDS) for rutin fatty ester with high mucus permeating properties. Int. J. Pharm. 562, 180–186. https://doi.org/10.1016/j.ijpharm.2019.03.036.

Charisiadis, P., Kontogianni, V., Tsiafoulis, C., Tzakos, A., Siskos, M., Gerothanassis, I., 2014. 1H-NMR as a structural and analytical tool of intra- and intermolecular hydrogen bonds of phenol-containing natural products and model compounds. Molecules 19, 13643–13682. https://doi.org/10.3390/molecules190913643.

Claus, V., Spleis, H., Federer, C., Zöller, K., Wibel, R., Laffleur, F., Dumont, C., Caisse, P., Bernkop-Schnürch, A., 2023. Self-emulsifying drug delivery systems (SEDDS): In vivo-proof of concept for oral delivery of insulin glargine. Int. J. Pharm. 639, 122964 https://doi.org/10.1016/j.ijpharm.2023.122964.

de Oliveira Vigier, K., García-Álvarez, J., 2017. Deep Eutectic and Low-Melting Mixtures, in: Bio-Based Solvents. Wiley, pp. 83–114. Doi: 10.1002/9781119065357.ch4.

Depalo, N., Corricelli, M., De Paola, I., Valente, G., Iacobazzi, R.M., Altamura, E., Debellis, D., Comegna, D., Fanizza, E., Denora, N., Laquintana, V., Mavelli, F., Striccoli, M., Saviano, M., Agostiano, A., Del Gatto, A., Zaccaro, L., Curri, M.L., 2017. NIR emitting nanoprobes based on cyclic RGD motif conjugated PbS quantum dots for integrin-targeted optical bioimaging. ACS Appl. Mater. Interfaces 9, 43113–43126. https://doi.org/10.1021/acsami.7b14155.

Emami, S., Shayanfar, A., 2020. Deep eutectic solvents for pharmaceutical formulation and drug delivery applications. Pharm. Dev. Technol. https://doi.org/10.1080/10837450.2020.1735414.

Fraguas-Sánchez, A.I., Fernández-Carballido, A., Martin-Sabroso, C., Torres-Suárez, A.I., 2020. Stability characteristics of cannabidiol for the design of pharmacological, biochemical and pharmaceutical studies. J. Chromatogr. B 1150, 122188. https://doi.org/10.1016/j.jchromb.2020.122188.

Fulmer, G.R., Miller, A.J.M., Sherden, N.H., Gottlieb, H.E., Nudelman, A., Stoltz, B.M., Bercaw, J.E., Goldberg, K.I., 2010. NMR chemical shifts of trace impurities: Common laboratory solvents, organics, and gases in deuterated solvents relevant to the organometallic chemist. Organometallics 29, 2176–2179. https://doi.org/10.1021/om100106e.

Gardouh, A.R., Nasef, A.M., Mostafa, Y., Gad, S., 2020. Design and evaluation of combined atorvastatin and ezetimibe optimized self- nano emulsifying drug delivery

system. J. Drug Deliv. Sci. Technol. 60, 102093 https://doi.org/10.1016/j.jddst.2020.102093.
Ghaedi, H., Ayoub, M., Sufian, S., Lal, B., Uemura, Y., 2017. Thermal stability and FT-IR analysis of Phosphonium-based deep eutectic solvents with different hydrogen bond donors. J. Mol. Liq. 242, 395–403. https://doi.org/10.1016/j.molliq.2017.07.016.
González-Rivera, J., Pelosi, C., Pulidori, E., Duce, C., Tiné, M.R., Ciancaleoni, G., Bernazzani, L., 2022. Guidelines for a correct evaluation of Deep Eutectic Solvents thermal stability. Curr. Res. Green Sustain. Chem. 5, 100333 https://doi.org/10.1016/j.crgsc.2022.100333.
Haider, M.B., Dwivedi, M., Jha, D., Kumar, R., Marriyappan Sivagnanam, B., 2021. Azeotropic separation of isopropanol-water using natural hydrophobic deep eutectic solvents. J. Environ. Chem. Eng. 9 https://doi.org/10.1016/j.jece.2020.104786.
Içten, E., Purohit, H.S., Wallace, C., Giridhar, A., Taylor, L.S., Nagy, Z.K., Reklaitis, G.V., 2017. Dropwise additive manufacturing of pharmaceutical products for amorphous and self emulsifying drug delivery systems. Int. J. Pharm. 524, 424–432. https://doi.org/10.1016/j.ijpharm.2017.04.003.
Jannin, V., Chevrier, S., Michenaud, M., Dumont, C., Belotti, S., Chavant, Y., Demarne, F., 2015. Development of self emulsifying lipid formulations of BCS class II drugs with low to medium lipophilicity. Int. J. Pharm. 495, 385–392. https://doi.org/10.1016/j.ijpharm.2015.09.009.
Jörgensen, A.M., Friedl, J.D., Wibel, R., Chamieh, J., Cottet, H., Bernkop-Schnürch, A., 2020. Cosolvents in self-emulsifying drug delivery systems (SEDDS): Do they really solve our solubility problems? Mol. Pharm. 17, 3236–3245. https://doi.org/10.1021/acs.molpharmaceut.0c00343.
Jurić, T., Uka, D., Holló, B.B., Jović, B., Kordić, B., Popović, B.M., 2021. Comprehensive physicochemical evaluation of choline chloride-based natural deep eutectic solvents. J. Mol. Liq. 343, 116968 https://doi.org/10.1016/j.molliq.2021.116968.
Knaub, K., Sartorius, T., Dharsono, T., Wacker, R., Wilhelm, M., Schön, C., 2019. A novel self-emulsifying drug delivery system (SEDDS) based on VESIsorb® formulation technology improving the oral bioavailability of cannabidiol in healthy subjects. Molecules 24, 2967. https://doi.org/10.3390/molecules24162967.
Kohli, K., Chopra, S., Dhar, D., Arora, S., Khar, R.K., 2010. Self-emulsifying drug delivery systems: An approach to enhance oral bioavailability. Drug Discov. Today. https://doi.org/10.1016/j.drudis.2010.08.007.
Kyriakoudi, A., Tsiouras, A., Mourtzinos, I., 2022. Extraction of lycopene from tomato using hydrophobic natural deep eutectic solvents based on terpenes and fatty acids. Foods 11, 2645. https://doi.org/10.3390/foods11172645.
Lam, H.T., Le, N.-M.-N., Phan, T.N.Q., Bernkop-Schnürch, A., 2021. Mucolytic self-emulsifying drug delivery systems (SEDDS) containing a hydrophobic ion-pair of proteinase. Eur. J. Pharm. Sci. 162, 105658 https://doi.org/10.1016/j.ejps.2020.105658.
Lee, H.-S., Tamia, G., Song, H.-J., Amarakoon, D., Wei, C.-I., Lee, S.-H., 2022. Cannabidiol exerts anti-proliferative activity via a cannabinoid receptor 2-dependent mechanism in human colorectal cancer cells. Int. Immunopharmacol. 108, 108865 https://doi.org/10.1016/j.intimp.2022.108865.
Li, H., Chang, S.L., Chang, T.R., You, Y., Wang, X.D., Wang, L.W., Yuan, X.F., Tan, M.H., Wang, P.D., Xu, P.W., Gao, W.B., Zhao, Q.S., Zhao, B., 2021. Inclusion complexes of cannabidiol with β-cyclodextrin and its derivative: Physicochemical properties, water solubility, and antioxidant activity. J. Mol. Liq. 334 https://doi.org/10.1016/j.molliq.2021.116070.
Lopedota, A.A., Arduino, I., Lopalco, A., Iacobazzi, R.M., Cutrignelli, A., Laquintana, V., Racaniello, G.F., Franco, M., la Forgia, F., Fontana, S., Denora, N., 2021. From oil to microparticulate by prilling technique: Production of polynucleate alginate beads loading Serenoa Repens oil as intestinal delivery systems. Int. J. Pharm. 599, 120412 https://doi.org/10.1016/j.ijpharm.2021.120412.
López-García, J., Lehocký, M., Humpolíček, P., Sáha, P., 2014. HaCaT keratinocytes response on antimicrobial atelocollagen substrates: Extent of cytotoxicity, cell viability and proliferation. J Funct Biomater 5, 43–57. https://doi.org/10.3390/jfb5020043.
Merrick, J., Lane, B., Sebree, T., Yaksh, T., O'Neill, C., Banks, S.L., 2016. Identification of psychoactive degradants of cannabidiol in simulated gastric and physiological fluid. Cannabis Cannabinoid Res. 1, 102–112. https://doi.org/10.1089/can.2015.0004.
Park, H., Ha, E.S., Kim, M.S., 2020. Current status of supersaturable self-emulsifying drug delivery systems. Pharmaceutics. https://doi.org/10.3390/pharmaceutics12040365.
Pereira, C.V., Silva, J.M., Rodrigues, L., Reis, R.L., Paiva, A., Duarte, A.R.C., Matias, A., 2019. Unveil the anticancer potential of limomene based therapeutic deep eutectic solvents. Sci. Rep. 9 https://doi.org/10.1038/s41598-019-51472-7.
Pisani, L., Iacobazzi, R.M., Catto, M., Rullo, M., Farina, R., Denora, N., Cellamare, S., Altomare, C.D., 2019. Investigating alkyl nitrates as nitric oxide releasing precursors of multitarget acetylcholinesterase-monoamine oxidase B inhibitors. Eur. J. Med. Chem. 161, 292–309. https://doi.org/10.1016/j.ejmech.2018.10.016.
Pouton, C.W., Porter, C.J.H., 2008. Formulation of lipid-based delivery systems for oral administration: Materials, methods and strategies. Adv. Drug Deliv. Rev. 60, 625–637. https://doi.org/10.1016/j.addr.2007.10.010.
Rengstl, D., Fischer, V., Kunz, W., 2014. Low-melting mixtures based on choline ionic liquids. PCCP 16, 22815–22822. https://doi.org/10.1039/C4CP02860K.
Roger, E., Gimel, J.-C., Bensley, C., Klymchenko, A.S., Benoit, J.-P., 2017. Lipid nanocapsules maintain full integrity after crossing a human intestinal epithelium model. J. Control. Release 253, 11–18. https://doi.org/10.1016/j.jconrel.2017.03.005.
Salawi, A., 2022. Self-emulsifying drug delivery systems: A novel approach to deliver drugs. Drug Deliv. 29, 1811–1823. https://doi.org/10.1080/10717544.2022.2083724.
Schaeffer, N., Abranches, D.O., Silva, L.P., Martins, M.A.R., Carvalho, P.J., Russina, O., Triolo, A., Paccou, L., Guinet, Y., Hedoux, A., Coutinho, J.A.P., 2021. Non-ideality in thymol + menthol type V deep eutectic solvents. ACS Sustain. Chem. Eng. 9, 2203–2211. https://doi.org/10.1021/acssuschemeng.0c07874.
Schellekens, R.C.A., Stuurman, F.E., van der Weert, F.H.J., Kosterink, J.G.W., Frijlink, H.W., 2007. A novel dissolution method relevant to intestinal release behaviour and its application in the evaluation of modified release mesalazine products. Eur. J. Pharm. Sci. 30, 15–20. https://doi.org/10.1016/j.ejps.2006.09.004.
Shah, P.A., Chavda, V., Hirpara, D., Sharma, V.S., Shrivastav, P.S., Kumar, S., 2023. Exploring the potential of deep eutectic solvents in pharmaceuticals: Challenges and opportunities. J. Mol. Liq. 390, 123171 https://doi.org/10.1016/j.molliq.2023.123171.
Smith, E.L., Abbott, A.P., Ryder, K.S., 2014. Deep eutectic solvents (DESs) and their applications. Chem. Rev. https://doi.org/10.1021/cr300162p.
Tang, W., Dai, Y., Row, K.H., 2018. Evaluation of fatty acid/alcohol-based hydrophobic deep eutectic solvents as media for extracting antibiotics from environmental water. Anal. Bioanal. Chem. 410, 7325–7336. https://doi.org/10.1007/s00216-018-1346-6.
Tran, P., Park, J.S., 2021. Recent trends of self-emulsifying drug delivery system for enhancing the oral bioavailability of poorly water-soluble drugs. J. Pharm. Investig. 51, 439–463. https://doi.org/10.1007/s40005-021-00516-0.
Turbiscan Stability Index: The Criteria and Correlation to Visual Observation [WWW Document], n.d. URL https://www.fullbrooksystems.co.uk/news/turbiscan-stability-index-the-criteria-and-correlation-to-visual-observation (accessed 1.17.24).
Van Osch, D.J.G.P., Dietz, C.H.J.T., Warrag, S.E.E., Kroon, M.C., 2020. The curious case of hydrophobic deep eutectic solvents: A story on the discovery, design, and applications. ACS Sustain. Chem. Eng. https://doi.org/10.1021/acssuschemeng.0c00559.
Wahlgren, C.-F., Quiding, H., 2000. Depth of cutaneous analgesia after application of a eutectic mixture of the local anesthetics lidocaine and prilocaine (EMLA cream). J. Am. Acad. Dermatol. 42, 584–588. https://doi.org/10.1067/mjd.2000.104303.
Watanabe, K., Itokawa, Y., Yamaori, S., Funahashi, T., Kimura, T., Kaji, T., Usami, N., Yamamoto, I., 2007. Conversion of cannabidiol to Δ9-tetrahydrocannabinol and related cannabinoids in artificial gastric juice, and their pharmacological effects in mice. Forensic Toxicol. 25, 16–21. https://doi.org/10.1007/s11419-007-0021-y.
Zaichik, S., Steinbring, C., Caliskan, C., Bernkop-Schnürch, A., 2019. Development and in vitro evaluation of a self-emulsifying drug delivery system (SEDDS) for oral vancomycin administration. Int. J. Pharm. 554, 125–133. https://doi.org/10.1016/j.ijpharm.2018.11.010.
Zainal-Abidin, M.H., Hayyan, M., Ngoh, G.C., Wong, W.F., Looi, C.Y., 2019. Emerging frontiers of deep eutectic solvents in drug discovery and drug delivery systems. J. Control. Release. https://doi.org/10.1016/j.jconrel.2019.09.019.
Zupančič, O., Rohrer, J., Thanh Lam, H., Grießinger, J.A., Bernkop-Schnürch, A., 2017. Development and in vitro characterization of self-emulsifying drug delivery system (SEDDS) for oral opioid peptide delivery. Drug Dev. Ind. Pharm. 43, 1694–1702. https://doi.org/10.1080/03639045.2017.1338722.